https://ntrs.nasa.gov/search.jsp?R=20180000002 2020-05-10T01:16:01+00:00Z

Paper ID: 7461

61st International Astronautical Congress 2010

Applications of Multi-Body Dynamical Environments: The ARTEMIS Transfer Trajectory Design

ASTRODYNAMICS SYMPOSIUM (C1)
Mission Design, Operations and Optimization (2) (9)

Mr. David C. Folta and Mr. Mark Woodard
National Aeronautics and Space Administration (NASA)/Goddard Space Flight Center, Greenbelt, MD, United States, david.c.folta@nasa.gov

Prof. Kathleen Howell, Chris Patterson, Wayne Schlei
Purdue University, West Lafayette, IN,
United States, howell@purdue.edu

Abstract

The application of forces in multi-body dynamical environments to permit the transfer of spacecraft from Earth orbit to Sun-Earth weak stability regions and then return to the Earth-Moon libration (L_1 and L_2) orbits has been successfully accomplished for the first time. This demonstrated transfer is a positive step in the realization of a design process that can be used to transfer spacecraft with minimal Delta-V expenditures. Initialized using gravity assists to overcome fuel constraints; the ARTEMIS trajectory design has successfully placed two spacecraft into Earth-Moon libration orbits by means of these applications.

INTRODUCTION

The exploitation of multi-body dynamical environments to permit the transfer of spacecraft from Earth to Sun-Earth weak stability regions and then return to the Earth-Moon libration (L_1 and L_2) orbits has been successfully accomplished. This demonstrated transfer is a positive step in the realization of a design process that can be used to transfer spacecraft with minimal Delta-Velocity (ΔV) expenditure. Initialized using gravity assists to overcome fuel constraints, the Acceleration Reconnection and Turbulence and Electrodynamics of the Moon's Interaction with the Sun (ARTEMIS) mission design has successfully placed two spacecraft into Earth-Moon libration orbits by means of this application of forces from multiple gravity fields.

Various design methods relying on multi-body dynamics were applied to achieve these transfers.[1,2,3,4,5] Generation of manifolds from dynamical information, optimization of forward numerically integrated states, and the selection of various trajectory conditions near various manifold structures were combined to ensure the design was successful given inherent modeling, navigation, and maneuver execution errors. The ARTEMIS design involves two distinct transfers, one for each spacecraft, which demonstrates the potential in the application. The design incorporated lunar gravity assists (one of which used a double gravity assist with a 13-day interval between lunar encounters), to archive the correct energy and orbital orientation to place the vehicles on the appropriate transfer arc. Having placed the spacecraft such that it can exploit the flow direction consistent with a Lissajous trajectory manifold to attain the final Earth-Moon orbital conditions, operational support then focused

on remaining near a manifold structure or a nearby manifold, given navigation errors and mismodeled perturbations as the flow shifts from dynamically stable to unstable modes.

Along this transfer trajectory, several maneuvers were executed, each adjusting the trajectory slightly, each converging to the chosen target of an Earth-Moon libration orbit insertion location at the desired epoch. These designs are very sensitive to mismodeled perturbations and to the maneuver errors. The paper addresses the lunar gravity assists, manifold generation, the optimization techniques as well as numerical solutions, sensitivity of the transfer, and the operational navigation solutions, and trajectory design implemented.

ARTEMIS Mission

The ARTEMIS mission was approved in May 2008 by NASA's Heliophysics Senior Review panel as an extension to the Time History of Events and Macroscale Interactions during Substorms (THEMIS) mission.[6,7,8] THEMIS encompasses five spacecraft in Earth orbit. The ARTEMIS mission involves moving the two spacecraft in the outer-most elliptical Earth orbits and, with lunar gravity assists, re-directing the spacecraft to both the L_1 and L_2 Earth-Moon libration point orbits via transfer trajectories that exploit the multi-body dynamical environment. The two spacecraft are denoted as P1 for the THEMIS B spacecraft and P2 for the THEMIS C spacecraft. The THEMIS team had long known that substantial orbit maneuvers would be necessary for the P1 and P2 spacecraft to avoid entering a deep umbra shadow that would drain all power from the batteries and put the spacecraft into a non-recoverable power state. At the request of the Principal Investigator (PI), analysts at the Jet Propulsion Laboratory (JPL) designed transfer trajectories for both P1 and P2 to insert them into Earth-Moon libration point orbits.[9] The maneuver plan included a series a propulsive Orbit-Raising Maneuvers (ORMs) to position each spacecraft for a series of lunar and Earth gravity assist maneuvers. The injections into the translunar orbits for P1 and P2 occurred in January and March 2010.

Once the Earth-Moon libration point orbits are achieved and maintained for several months, both P1 and P2 will be inserted into elliptical lunar orbits. The current baseline is a two-year mission with departure maneuvers that began in June 2009, and targeted multiple lunar flybys in February 2010 that eventually place the spacecraft on the transfer trajectory. The P1 spacecraft entered the Earth-Moon L_2 Lissajous orbit on August 25, 2010 and the P2 spacecraft will follow October 23, 2010. In early April of 2011, both spacecraft will be transferred into highly elliptical lunar orbits. ARTEMIS will use simultaneous measurements of particles and electric and magnetic fields from two locations to provide the first three-dimensional information on how energetic particle acceleration occurs near the Moon's orbit, in the distant magnetosphere, and in the solar wind. ARTEMIS will also collect unprecedented observations of the refilling of the space environment behind the dark side of the Moon – the greatest known vacuum in the solar system – by the solar wind.

As a final multi-body mission goal, ARTEMIS will be the first spacecraft to navigate to and perform stationkeeping operations around the Earth-Moon L_1 and L_2 Lagrangian points. The NASA Goddard Space Flight Center (GSFC) has previous mission experience flying in the Sun-Earth L_1 (SOHO, ACE, WIND, ISEE-3) and L_2 regimes (WMAP, ISEE-3) and have maintained these spacecraft in libration point orbits by performing regular orbit stationkeeping maneuvers. The ARTEMIS mission will build on these experiences, but stationkeeping in Earth-Moon libration orbits presents new challenges since the libration point orbit period is on the order of two weeks rather than six months. As a result, stationkeeping maneuvers to maintain the Lissajous orbit will need to be performed frequently, and the orbit determination solutions between maneuvers will need to be quite accurate. Further information on this currently operational phase of the mission will be provided in the future.

ARTEMIS Partnership

NASA's Goddard Space Flight Center's Navigation and Mission Design Branch (NMDB), code 595, is currently supporting the ARTEMIS mission and will be prime for Earth-Moon libration point orbit navigation, trajectory design, maneuver planning, and command information generation. The ARTEMIS mission is a collaborative effort between NASA GSFC, the University of California at Berkeley (UCB), and the Jet Propulsion Laboratory (JPL). JPL provided the reference transfer trajectory plan from the elliptical orbit phase using a single impulsive maneuver to achieve the lunar gravity assist with one deterministic maneuver through libration orbit insertion. The Mission Operations Center (MOC) at the University of California at Berkeley (UCB) provides spacecraft operations support for ARTEMIS. Tracking, telemetry, and command services are provided using the S-band frequency via various networks, including the Berkeley Ground Station (BGS), the Universal Space Network (USN), the NASA Ground Network (GN) and Space Network (SN). UCB provides daily monitoring and maintenance of all spacecraft operations and the generation of maneuver commands for uploads using GSFC developed software.

ARTEMIS Spacecraft Overview

Each ARTEMIS spacecraft is spin-stabilized with a nominal spin rate of roughly 20 RPM. Spacecraft attitude and rate are determined using telemetry from a Sun sensor (SS), a three-axis magnetometer (TAM) used near Earth perigee, and two single-axis inertial rate units (IRUs). The propulsion system on each spacecraft is a simple monopropellant hydrazine blow-down system. The propellant is stored in two equally-sized tanks and either tank can supply propellant to any of the thrusters through a series of latch valves. Each observatory was launched with a dry mass of 77 kg and 49 kg of propellant, supplying a wet mass of 126 kg at beginning of life.

Each spacecraft has four 4.4 Newton (N) thrusters – two axial thrusters and two tangential thrusters. The two tangential thrusters are mounted on one side of the spacecraft and the two axial thrusters are mounted on the lower deck, as seen in Figure 1. The thrusters fire singly or in pairs – in continuous or pulsed mode – to provide orbit, attitude, and spin rate control. Orbit maneuvers can be implemented by firing the axial thrusters in continuous mode, the tangential thrusters in pulsed mode, or a combination of the two (beta mode). Since there are no thrusters on the upper deck, the combined thrust vector is constrained to the lower hemisphere of the spacecraft.

ARTEMIS Spacecraft Maneuvers Constraints

The ARTEMIS spacecraft are spinning vehicles with the spin axis pointed within 5 degrees of the south ecliptic pole. These spacecraft can implement a ΔV (thrust direction) along the spin axis towards the south ecliptic pole direction or in the spin plane, but cannot produce a ΔV in the northern hemisphere relative to the ecliptic. While the axial thrusters can be used if necessary, these thrusters are not calibrated as well as the radial thrusters. This constraint limited the location of maneuvers and these maneuvers were performed in a radial direction. For the lunar gravity assist and the multi-body dynamical environment, the trajectory was optimized using a nonlinear constraint that placed the ΔV in the spin plane. The maneuver epoch was also varied to yield an optimal radial maneuver magnitude.

In addition to the direction of maneuvers, another 'error' source also resulted in some interesting maneuver planning. This is the fact that, as a spinning spacecraft, a maneuver will be quantized into ~ 2 cm/s intervals with a start time that is dependent upon the Sun pulse in each spin. This meant that there was a finite maneuver accuracy that could be achieved that was dependent upon the ΔV magnitude for each maneuver. Some maneuvers could be quantized by varying the maneuver epoch, but DSN coverage often led to this method not being easily enacted. Thus many maneuvers are taken with the associated errors from spin pulse and timing. Table 1 shows the ARETMIS thruster firing modes.

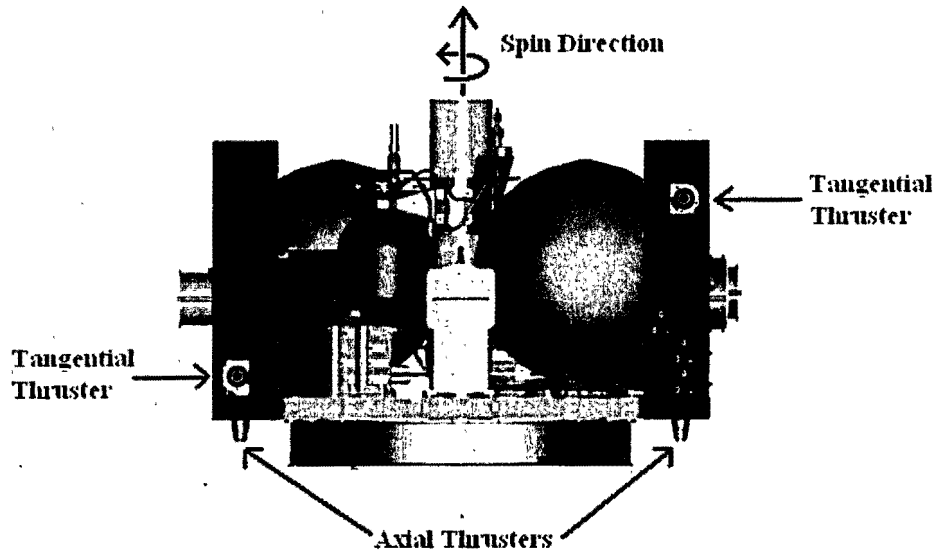

Figure 1. ARTEMIS Spacecraft Bus Design.

Table 1. ARTEMIS Thruster Firing Modes

Thruster Firing Modes			
Maneuver Type	Thrusters Involved	Depiction of Operational Mode	Purpose of Maneuver
Axial Thrust	A1 and A2 continuous firing		Perigee or apogee change or combined in-plane and out-of-plane orbit change with stowed EFI booms
Side Thrust	T1 and T2 pulsed firing		Perigee or apogee change with deployed EFI booms
Beta Thrust	A1 and A2 continuous firing alternating with T1 and T2 pulsed firing		In-plane and out-of-plane orbit change with deployed EFI booms
Attitude Precession	A1 or A2 pulsed firing		Attitude change
Spin-up / Spin-down	T1 or T2 continuous or pulsed firing		Spin rate adjustment

TRAJECTORY DESIGN

The ARTEMIS trajectory designs are illustrated in Figures 2 and 3. The two diagrams show the ARTEMIS P1 and P2 trajectories in the Sun-Earth rotating frame during the translunar phase. These general designs were originally determined using a dynamical process with a software tool called LTOOL.[10] During operations, this phase began with a carefully planned series of Orbit-Raising Maneuvers (ORMs) performed near periapsis to methodically raise apoapsis to lunar distance. The ORMs are carefully timed to phase the final apoapsis approach with lunar approach to achieve a lunar gravity assist maneuver. Gravity assists are a key component of the ARTEMIS trajectory design, as neither spacecraft has sufficient propellant to perform a direct insertion into the Earth-Moon libration point orbits. During the last few orbits prior to the lunar encounter, small Lunar Targeting Maneuvers

(LTMs) and Trajectory Correction Maneuvers (TCMs) corrected for maneuver execution errors during the last ORMs and align the lunar approach trajectory to the proper B-plane targets.

Multi-Body Dynamical Environment Phase

Following the first close lunar gravity assist, the P1 spacecraft flies under the Earth and performs a second gravity assist roughly 13 days later, as seen in the Sun-Earth rotating frame in Figure 2. A Deep Space Maneuver (DSM1) was performed 33 days later. DSM1 targets through Earth peraispsis and to the Earth-Moon libration insertion state. Following the Earth periapsis, the P1 spacecraft once again transfers into the general vicinity of the Sun-Earth L_1 Lagrangian point. This region is also identified as a "weak stability boundary" region. At the final bend in the P1 trajectory, the spacecraft is at a maximum range of 1.50 million km from the Earth. At this point, the trajectory begins to fall back towards the Earth-Moon system. A second deep space maneuver (DSM2) targets the Earth-Moon L_2 Lagrangian point. A large Lissajous Insertion Orbit (LOI) maneuver will be performed to insert P1 into the proper L_2 Lissajous orbit. The P2 translunar trajectory uses a single lunar swingby and three deep space maneuvers, two Earth periapses, and the Lissajous orbit insertion maneuver.

For both P1 and P2, we have allocated 4% of the total propellant budget to perform any required trajectory correction maneuvers (TCMs) along the way. The trajectory design focused on achieving the Earth-Moon libration insertion conditions to permit the final stage of the ARETMIS mission, which includes a Lissajous orbit with a transfer to a high eccentric lunar orbit. Following the lunar flyby targeting phase that included several flybys at ranges from 50,000km to just over 11,000km, the transfer trajectory began. The flyby targets were required to enable the energy to place the ARTEMIS spacecraft near the appropriate outgoing manifolds. Since the two spacecraft were originally designed for a different mission, a highly elliptical Earth orbit, and were already flying, fuel was (and is) extremely limited. Thus, with the unique operational constraints, accomplishment of the transfer goals with the minimum cost in terms of fuel is the highest priority.

Perturbation Model Fidelity

A full ephemeris model (DE405 file) was used which incorporated point mass gravity representing Earth, Moon, Sun, Jupiter, Saturn, Venus, and Mars. Also included is an eighth degree and order Earth potential model. The solar radiation pressure force is based on the measured spacecraft area and the estimated mass (from bookkeeping) and the coefficient of reflectivity from navigation estimation. The trajectory simulations are based on a variable step Runge-Kutta 8/9 and Prince-Dormand 8/9 integrator. The libration point locations are also calculated instantaneously at the same integration interval. Initial conditions used thoughtout the maneuver planning process correspond to the UCB delivered navigation solutions using both the DSN and the UCB tracking system. While several coordinates systems are used, the baseline ARTEMIS mission specified Earth Centered Cartesian (J2000) coordinates and an Earth-Moon rotating system are used. Software tools used in this process include the General Mission Analysis Tool (GMAT) developed at GSFC as an open source high fidelity tool with optimization and MATLAB® connectivity and AGI's STK/Astrogator suite.

Optimization of Maneuvers

To compute maneuver requirements in terms of ΔV, our strategy involves various numerical methods: traditional Differential Corrections (DC) targeting with central or forward differencing and optimization using the VF13AD algorithm from the Harwell library. A DC process provides for an a-priori condition and is also used for verification of the ΔV magnitude and direction. For the DC, equality constraints are incorporated, while for optimization, nonlinear equality and inequality constraints are employed. These constraints incorporate both the desired target conditions at the Earth-Moon system as well as the spacecraft constraints on the ΔV direction and relationship between the spin axis and the ΔV vector.

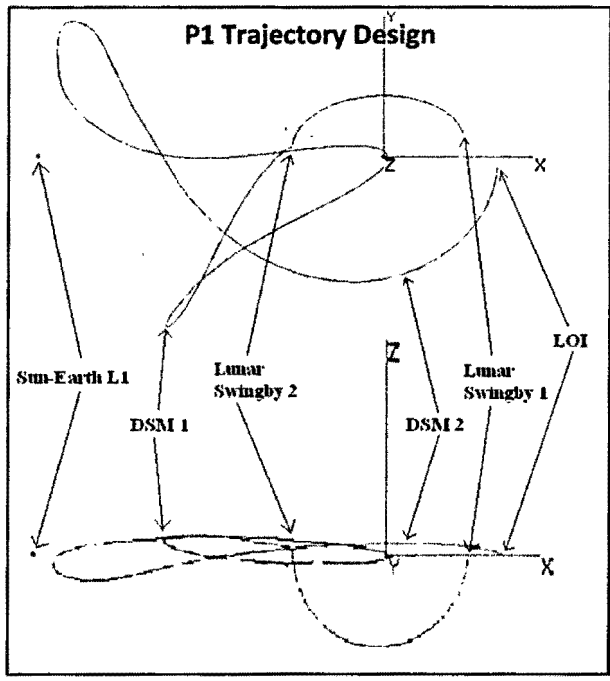

Figure 2. ARTEMIS P1 Trajectory Design

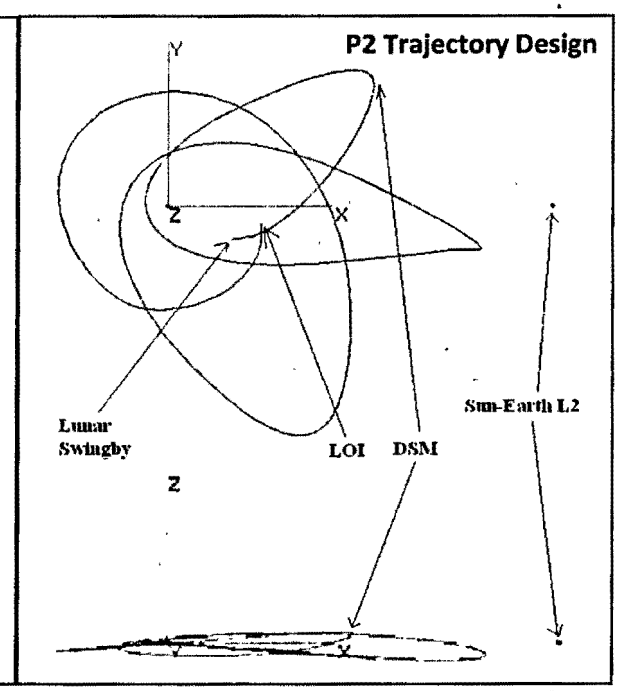

Figure 3. ARTEMIS P2 Trajectory Design

EM-Libration Insertion Targets

The end goal of the transfer phase was to achieve the Earth-Moon Lissajous insertion conditions necessary for a minimal energy insertion into the Earth-Moon L_2 or L_1 Lissajous orbits. The goals were defined in terms of the Earth J2000 Coordinates. These targets were held constant over the entire mission design process. As part of the early design process, a minimum ΔV was necessary since the bulk of the fuel had been used in the prime science mission. This left the designers with a fuel budget that could get them to the Moon directly, but without the required fuel to insert into lunar orbit. Although a baseline trajectory is defined to design the mission, there is no true reference motion that is required.

Navigation Uncertainties

Throughout the entire trajectory design process, navigation solutions were generated at a regular frequency of once every three days with the exception of post maneuver navigation solutions which were made available once a converged solution was determined. The rapid response was to ensure that the maneuver had performed as predicted and that no unanticipated major changes to the design were necessary. Table 2 includes a list of the major navigation solutions used in maneuver planning and their uncertainties. As seen, the RSS of the uncertainties are on the order of 10s of meters in position and below 1 cm/s in velocity. As a conservative estimate for maneuver planning and error analysis, 1σ uncertainties of 1 km in position and 1 cm/s in velocity are used. These accuracies were obtained using nominal tracking arcs of one three-hour contact every other day. This frequency of contacts was investigated earlier in the mission design process and was thought to meet the accuracy goals as stated above. The Goddard Trajectory Determination System (GTDS) is used for all navigation estimation.

Table 2 – Sample Navigation Solution Uncertainties per Phase during Transfer Trajectory

Phase	Navigation Arc Length (days)	Position Accuracy (m) (1σ)	Velocity Accuracy (cm/s) (1σ)
P1 Deep Space	21	34	0.09
P1 TCM5	7	43	0.11
P2 Deep Space	13	12	0.04
P2 TCM1	23	51	0.02

END-TO-END TRAJECTORY DESIGN

The transfer trajectory design approach uses both the numerical methods as discussed above with the inclusion of dynamical systems for verification and to gain knowledge of the transfer dynamics. The transfers were implemented as designed and, then, knowledge of the Sun-Earth/Moon dynamics was applied to verify that the target conditions would be met. The spacecraft were targeted to the libration point orbit insertion location knowing full well that maneuver execution and navigation errors would push the path off the 'baseline' design. A correction maneuver was planned that would essentially shift the trajectory, such that the new path would be consistent with a nearby manifold or the expected flow in this regime. An established method of calculating a manifold is the determination of the stable or unstable mode direction associated with a Sun-Earth or an Earth-Moon Lissajous trajectory via the monodromy matrix, then using an off-set at an appropriate location along the Lissajous trajectory, integrating forward or backward along the stable or unstable direction. An intersection of the resulting manifold with the 'current' trajectory can be used to identify a likely maneuver location and is frequently the basic strategy employed to visualize the flow. While this approach has previously been successfully applied for maneuver planning, and was initially investigated as a means to determine a location of the maneuver here, it was decided that a forward integrating numerical optimization process would be a better fit with respect to the spacecraft constraints for the purpose of calculating optimized ΔV s. This optimization procedure permitted minimization of the ΔV magnitude, variation of the ΔV components in azimuth, as well as variation of the maneuver epoch, while incorporating the nonlinear constraint on the spacecraft ΔV direction relative to the spin axis. The manifold computations supplied the intuitive design but could not be used effectively at this point to also constrain the maneuver directions. An example of two manifolds as applied to the ARTEMIS P1 trajectory design appears in Figure 4. The left plot represents the computation of stable manifolds progressing towards a Sun-Earth L_1 Lissajous trajectory and illustrates (in red) a local manifold originating at the post-DSM position along the path and arriving in the vicinity of the Sun-Earth L_1 Lissajous orbit. The figure (right side) reflects unstable manifolds that depart from the Sun-Earth L_1 Lissajous trajectory, illustrating a local manifold (in red) that flows towards the point along this Sun-Earth unstable manifold that reaches the Earth-Moon L_2 Lissajous entry region, that is, it approaches the stable manifold associated with Earth-Moon L_2 Lissajous trajectory. The trajectory design reflects the merger of these two local manifolds to complete the mission (that is, the unstable manifold from the Sun-Earth L_1 region to blend into the stable manifold that delivers the vehicle to the Earth-Moon L_2 vicinity). For flow information to serve as a basis for the P2 transfer, the stable manifolds associated with the Earth-Moon L_2 Lissajous trajectory were propagated backwards and transformed directly to the Sun-Earth coordinate frame; the P2 path blended into the flow consistent the Earth-Moon manifolds directly from the relatively large DSM maneuver.

In reality, as the TCM maneuvers were performed, the path essentially jumped from the vicinity of one local manifold to another, at a slightly different energy level, to manage both the trajectory design and the mission constraints. The manifolds realized were generated using the initial condition (post-maneuver). To ensure that a verifiable trajectory solution was realized, the optimized maneuver solutions

were correlated with these manifolds. Another focus of the paper is to demonstrate that the number of optimized maneuvers was very low and their magnitudes quite small, considering the sensitivity of the dynamics and uncertainties of the OD solutions.

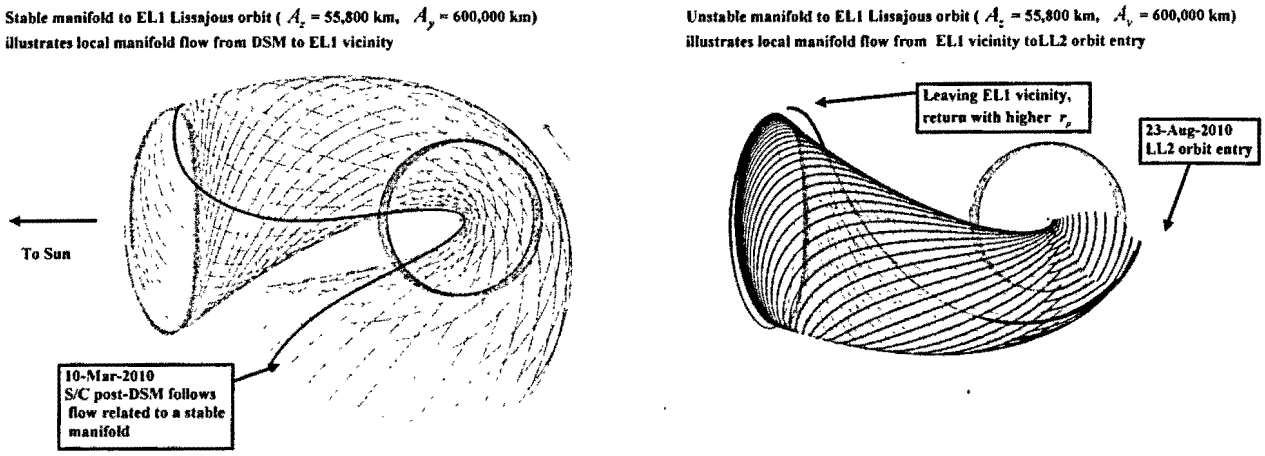

Figure 4. Baseline P1 Out-Bound to Max Radius on Stable Manifold and In-Bound to Lissajous Orbit on Unstable Manifold

Optimal ΔV Maneuver Design and Placement

As the transfer trajectory was flown, correction maneuvers were required to adjust for maneuver execution errors as a result of the previous maneuver, the spacecraft pointing and implementation errors, as well as the navigation errors. These maneuvers, called Trajectory Correction Maneuvers (TCM), represent the statistical maneuvers along the transfer. A deterministic maneuver included in both the P1 and P2 design was called a Deep Space Maneuver (DSM), to separate it from maneuvers that were performed while in the elliptical orbit, which raised the aposapsis and eventually targeted the lunar gravity assists.

To target to the desired Earth-Moon Lissajous conditions, a VF13AD optimizer was used that incorporated the following variables and constraints. The values listed in the Table 3 are representative control parameters for the correction maneuvers. These values can vary by a factor of ten, depending on the sensitivity of the trajectory. Table 4 lists sample P1 targeted states, epoch, and angle information wrt the spin axis. These targets where held constant throughout the transfer optimization.

Table 3. Sample Optimization Control Variables

Control Variable	Max perturbation (days or m/s s)	Max Stepsize (days or m/s)
Maneuver Epoch	.01	0.5
ΔV X -component	1e-8 to 1e-10	1e-3 to 1e-5
ΔV Y -Component	1e-8 to 1e-10	1e-3 to 1e-5
ΔV Z -Component	1e-8 to 1e-10	1e-3 to 1e-5

Table 4. Sample Linear and Non-Linear Constraints

Target / Constraint	Earth-Moon L2 Goals (in Earth J2000 Coord)	Tolerance
X position	352031 km	1 km
Y position	-318469 km	1 km
Z position	-131402 km	1 km
Julian Date Epoch	2455431.500	60 sec
Non-linear: ΔV angle wrt Spin Axis	89 deg	.05 deg

At each maneuver location, the optimizer was run to determine the minimal ΔV location. To determine an a priori maneuver location and to achieve an intuitive feel for the maneuver results, a DC process was performed which anticipated maneuver locations based on DSN coverage. Table 5 includes the P1 spacecraft maneuver information for all the post-DSM transfer trajectory maneuvers. In Table 6, the P2 spacecraft maneuver information is listed for all the transfer trajectory maneuvers. Note that TCM numbers originate at '1', reflecting the corrections performed only in the multi-body dynamical environment phase. For P1, maneuvers TCM1 through TCM4 were completed in the elliptical orbit or during lunar gravity assist targeting. As shown in Tables 5 and 6, the maneuver execution errors are small at only a few percent. These errors are a function of actual start time wrt a sun pulse of a spinning spacecraft, tank temperatures, attitude knowledge, and the general propulsion system performance

Table 5. P1 Trajectory Correction Maneuvers

Maneuver	Epoch (UTCG)	ΔV Magnitude (m/s)	Final Maneuver Error (%)	Reason for Maneuver
DSM	March 10, 2010 @ 19:00	7.30	1.46	Deterministic DV
TCM 5	April 20, 2010 @ 09:00	0.18	-2.06	DSM Correction
TCM 6	June 20, 2010 @ 21:45	0.18	-3.24	TCM 5 Correction
TCM 7	July 19, 2010 @ 23:00	0.66	0.61	Arrival Epoch
TCM 8	August 18, 2010 @ 06:00	1.90	n/a	Arrival Epoch

Table 6. P2 Spacecraft maneuver information

Maneuver	Epoch (UTCG)	ΔV Magnitude (m/s)	Final Maneuver Error (%)	Reason for Maneuver
TCM 1	March 26, 2010 @ 02:05	0.65	-0.60	Lunar Flyby Correction
DSM I	May 13, 2010 @ 02:21	3.68	-3.43	Deterministic DV
DSM 2	June 1, 2010 @ 14:50	24.25	-0.57	Deterministic DV
TCM 2	July 20, 2010 @ 12:00	2.22	0.28	DSM 2 Correction
TCM 3	August 2, 2010 @ 12:00	0.64	1.90	DSM 1&2 Correction
DSM 3 (proposed)	September 13, 2010	1.63	n/a	Arrival Epoch and EM L_1 Z-Evolution

Figures 5 and 6 show the locations of the P1 and P2 maneuvers during the multi-body dynamical environment phase in each case. The maneuvers compensate for the maneuver execution errors, the

navigation errors, and the subsequent maneuvers to correct for these errors. These errors and small mis-modeled perturbations can lead not only to late or early arrival times at the prescribe Lissajous insertion location, but also contribute to out-of-plane affects and may result in trajectories that intersect with the Moon. Clearly, the trajectory is very sensitive to such small perturbations. But, that sensitivity also implies that small corrections can alter the trajectory design significantly and allow fine control.

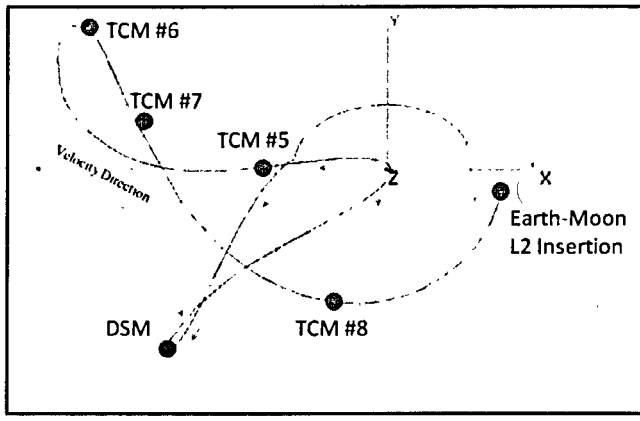

Figure 5. P1 Maneuver Locations

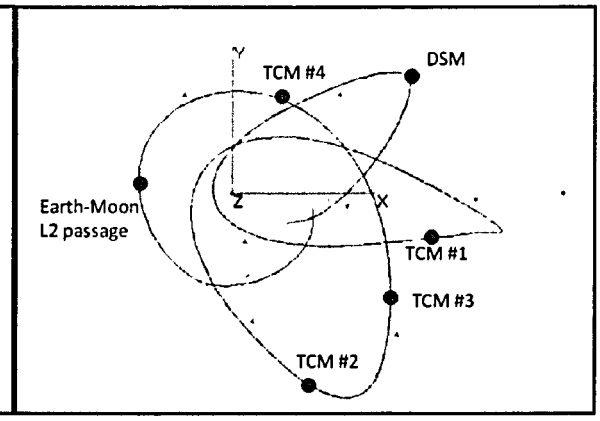

Figure 6. P2 Maneuver Locations

The numerically generated trajectories for two maneuvers, the DSM and TCM5, appear in Figure 7 as they were executed. Note how the resulting (post maneuver) trajectory varied due to maneuver execution and navigation errors as well as any mismodeling in solar radiation pressure. The largest difference is shown in the post-DSM trajectory as the maneuver error was significant at 11 cm/s. In the TCM5 maneuver used to correct the DSM error, the resultant accuracy yielded an error of 0.4 cm/s. This error was corrected in the TCM 6 maneuver. Two additional TCM maneuvers were then executed to adjust the arrival epoch into the Earth-Moon entry point and subsequent Lissajous trajectory. These time change maneuvers were required to permit the correct z amplitude-evolution in both the L_2 and L_1 orbits. Recall that the z frequency is not correlated with the in-plane frequency, thus, a change to the Lissajous insertion time provides a method to adjust the initial velocities and Z component amplitudes. Figure 8 presents the P2 trajectory for the optimized DSM and the correction TCM. As is apparent, the trajectory diverges after approximately one revolution around Earth, where the orbit radius is beyond the lunar orbit radius. In contrast, the corrected trajectory passes by the L_2 side using a half-Lissajous and then transfers to the Earth-Moon L_1 side

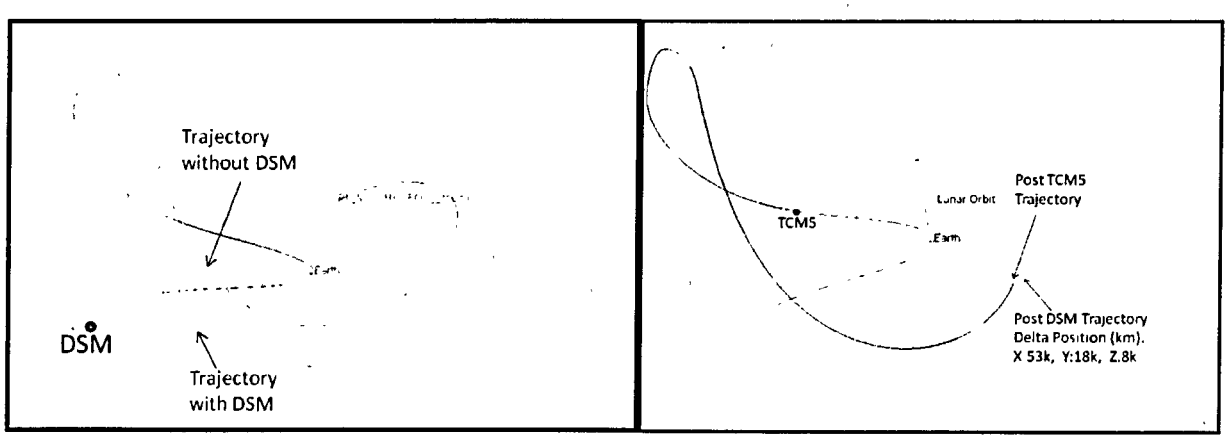

Figure 7. Preplanning and Optimized P1 DSM and Post-DSM and Optimized TCM5 Trajectory

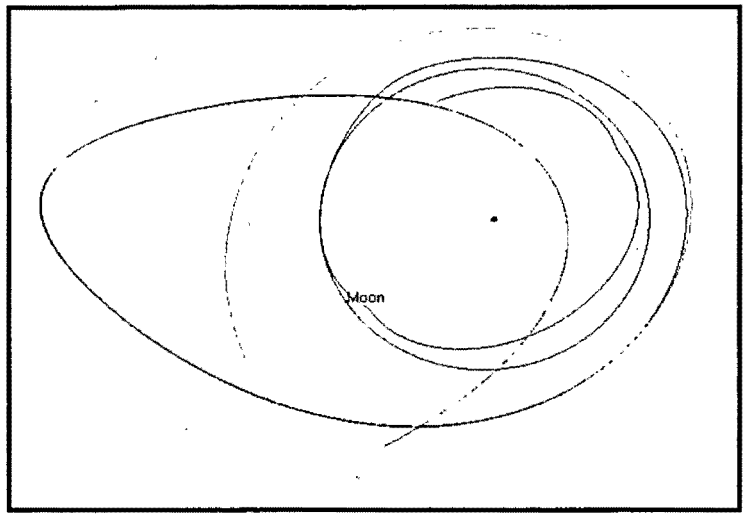

Figure 8. Post P2 DSM and Optimized TCM3 Trajectory

MULTI-BODY DYNAMICAL ENVIRONMENT MANIFOLDS

Before discussing the flow in the multi-body dynamical environment that correlates with the ARTEMIS transfer path, a brief definition of a manifold is offered.[11,12,13,14,15,16] For this application, a manifold is a representation of local trajectories that are subsequently numerically integrated in a full ephemeris model. Additionally, 'manifolds' are frequently represented either by the numerical results, by algorithms that define the state-space via lower-fidelity circular restricted modeling, or even by continuously differentially corrected arcs. The manifolds plotted in this paper are constructed using the initial and ephemeris states of the optimal or actual navigation solutions, meaning they represent a higher-fidelity model of all local (nearby) trajectories.

For ARTEMIS, manifolds that exist in the multi-body dynamical environment were generated to verify the numerically integrated, optimally planned, and actual post-maneuver results. The computation of manifolds also demonstrates the design process that can potentially shift a trajectory arc from the vicinity of one manifold to another and, thus, attain the targeted Lissajous insertion states (that is, an L_2 state for the P1 spacecraft and an L_1 state for the P1 spacecraft). These manifold computations are used essentially to interpret the effects of the DSM and the TCM maneuvers and to illustrate how the stable or unstable manifolds do, in fact, intersect near the maneuver locations. Manifolds are plotted for the pre- and post-DSM and TCM5 maneuvers of the P1 spacecraft and for the pre- and post-DSM trajectory arcs for the P2 spacecraft. In Figure 9, the P1 stable manifold appears, to reflect the actual trajectory as designed, for the optimal condition that would permit P1 to coast throughout the trajectory to the point of maximum excursion; subsequently, the spacecraft would closely follow the flow consistent with an unstable manifold to eventually arrive at the L_2 insertion location. But, as with all maneuvers and operations, errors in maneuver execution and navigation error affect the results. As noted, for the P1 spacecraft, two manifolds are actually used to represent the behavior of the system, i.e., the stable manifold which traverses the outbound trajectory and the unstable manifold which provides a path to deliver the spacecraft to the Earth-Moon Lissajous orbit insertion state. But, for now, consider only the outbound arc and TCM5. From the DSM, P1 follows the original outbound path to the location of TCM5. Note that, if TCM 5 is to be implemented, the maneuver will shift the spacecraft to a different path, one that can be envisioned in terms of a different manifold. Subsequent to the DSM, and along the outbound trajectory, then, two outbound manifold arcs emerge from the TCM5 location and are plotted in Figures 9, 10, and 12. These two manifolds represent the potential outcomes from (1) flow along the

optimal path and (2) the alternative that incorporates a possible TCM5 maneuver. Figure 9 presents the optimal (planned) DSM manifold. Note the location of the potential TCMs in this design. Figure 10 reflects the maneuver effect of an exaggerated TCM5 applied to correct for a DSM execution error and demonstrates the P1 'jump' from the vicinity of one stable manifold (green) to an alternate transfer path that is represented by flow along another manifold (orange). An exaggerated view appears in Figure 11 to highlight this manifold jump and visualize the shift in the flow directions that can result from a maneuver. For ARTEMIS, the manifolds were not directly incorporated to determine the optimal maneuver locations but to assess the feasibility and dynamical foundation of the overall structure of the design. Manifold intersections as part of the design process to determine maneuver locations can be done and has been proven both in research and in operations for the Genesis mission.[17,18] The P1 unstable manifold and the effect of TCM5 on the return portion of the orbit are plotted in Figure 12 for an exaggerated TCM5 maneuver. The figure includes the original planned and the corrected post TCM5 trajectory. For the actual, relatively small TCM5 maneuver, the difference is slight in terms of the larger design but the shift in the general direction of the flow is consistent with a new manifold; the post TCM5 path with a small shift in direction guaranteed that P1 would reach its goal at the proper epoch.

The actual path for the P2 spacecraft (blue) as well as a computed manifold surface (green) appears in Figure 13. This manifold design reflects the corrected manifolds to deliver the vehicle directly from the DSM to the vicinity of the Earth-Moon Lissajous stable manifold. Off-nominal conditions require a maneuver that shifts to the vicinity of this same manifold to successfully arrive at the Earth-Moon Lissajous orbit. Similar to the P1 design, the manifold is used to verify the feasibly of the optimized correction maneuver. The P2 spacecraft also jumps or shifts from the vicinity of one manifold to flow in a direction consistent with the required manifold at the maneuver location.

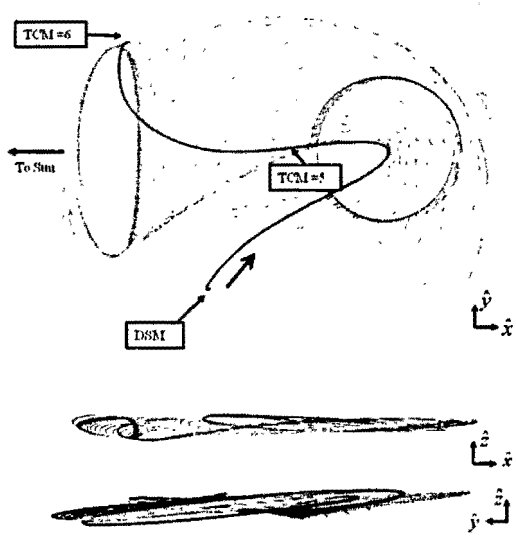

Figure 9. P1 Planned Stable Sun-Earth Manifold

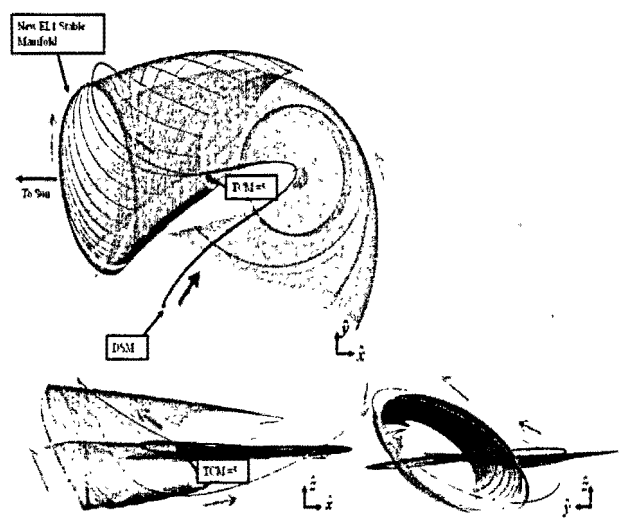

Figure 10. P1 Pre and Post TCM5 Stable Sun-Earth Manifold

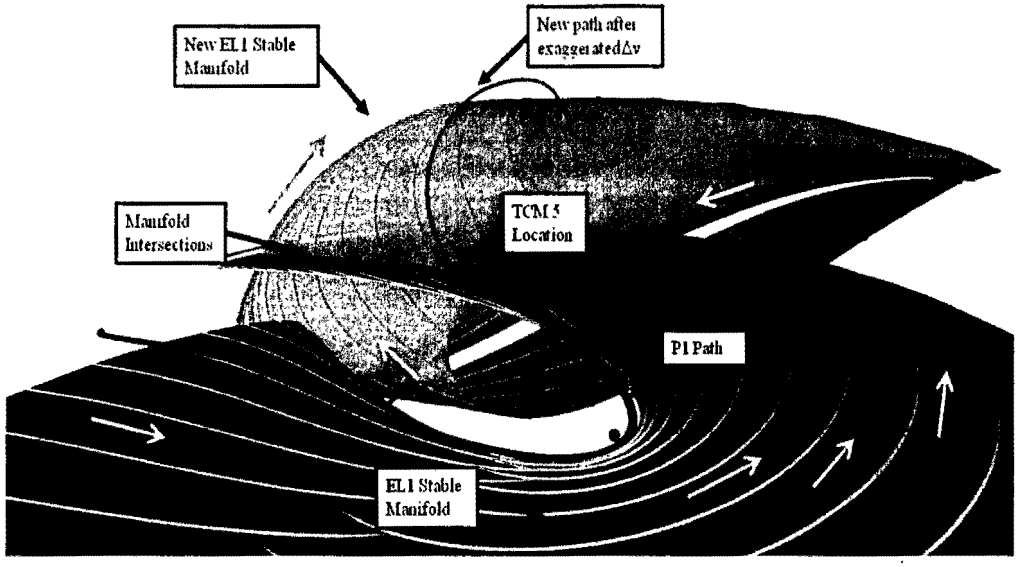

Figure 11. Exaggerated Post DSM and Post TCM5 P1 Stable Manifolds

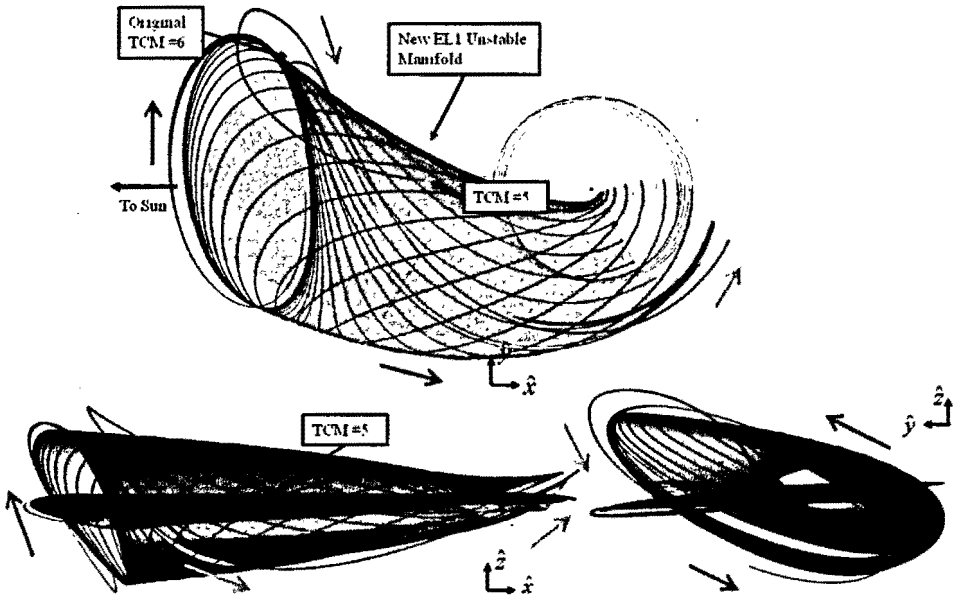

Figure 12. P1 Post TCM5 Unstable Manifold to L_2 Lissajous Targeted State

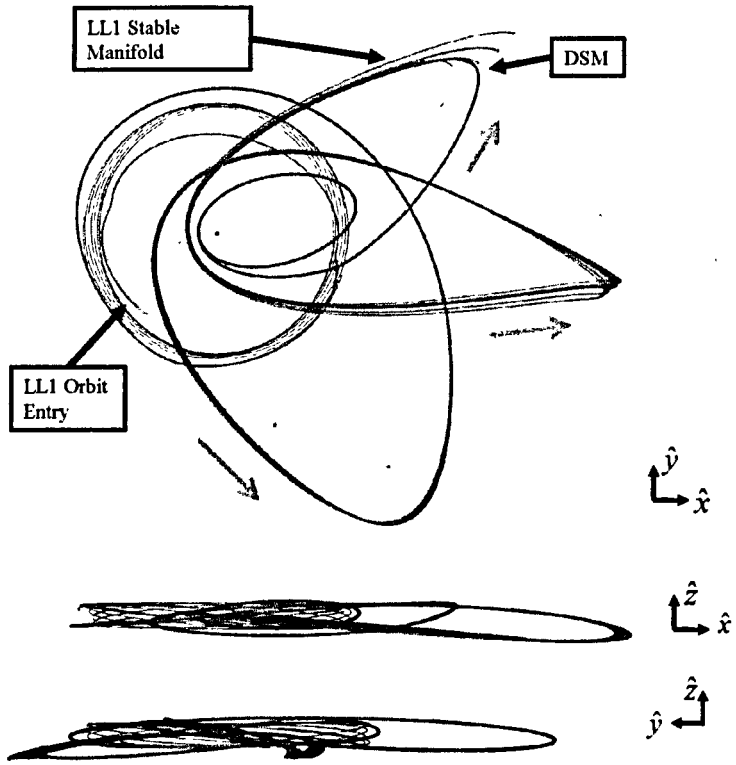

Figure 13. P2 Manifold

SUMMARY

The ARTEMIS mission provided many challenges and opportunities. The challenges of the spacecraft constraints, the multi-body dynamical environment, and the navigation performance can be overcome by the judicious use of optimization tools and manifold generation for verification. Several reliable software tools were available to permit cross checking of all maneuver plans and predicted trajectories. The overall sensitivity of the trajectory to the dynamical environment was found to be near the anticipated levels as those proposed from many theoretical investigations and from recent operational missions that briefly flew trajectories which passed thought these multi-body dynamical environments. Small errors produced a large effect on the transfer design, but small, well-placed maneuvers can also correct these errors. While there are a number of strategies available that incorporate the Earth-Moon dynamics, the actual mission applications and mission constraints must also be considered. The methods developed here allow a general application whether there is a reference orbit, spacecraft constraints on ΔV direction, or orbital parameters requirements. The required transfer ΔV budget can be minimized and the capability to reduce the budget to a very low level is substantially enhanced by exploiting the dynamical structure.

CONCLUSIONS

The ARTEMIS mission is an absolute success and this success can be attributed to the use of several tools to validate and confirm the planning and execution of maneuvers necessary to transit a dynamically challenging environment. The combined method of optimization with manifold verification, thought not new, is a substantial leap in the operational design of such missions. With the completion of the ARTEMIS trajectory, a viable multi-tiered process and trajectory feasibility is demonstrated. The opportunities of the ARTEMIS mission provide the space community with the first ever completed

design from Earth to the Earth-Moon L_2 and L_1 Lissajous orbits. The ARTEMIS P1 spacecraft has completed its transfer and is in now in the Earth-Moon L_2 Lissajous trajectory; the P2 spacecraft is on-track for Earth-Moon libration orbit insertion.

ACKNOWLEDGEMENTS

The authors would like to acknowledge Dan Cosgrove, Manfred Bester, Sabine Frey, and all the operations personnel at the University of California Berkeley. Their operational expertise and open communications ensured a successful mission. Also, we would like to thank our JPL colleagues; Steve Broschart, Ted Sweetser, and Greg Whiffen for their outstanding baseline concept and assistance in planning and executing the aforementioned maneuvers.

REFERENCES

1. Folta, D., Vaughn, F., "A Survey of Earth-Moon Libration Orbits: Stationkeeping Strategies and Intra-Orbit Transfers," Paper No. IAC-02-Q.6.08, 53rd International Astronautical Congress, World Space Congress, Houston, Texas, October 10-19, 2002.

2. Howell, K.C., and Gordon, S.C., "Orbit Determination Error Analysis and a Station-Keeping Strategy for Sun-Earth L_1 Libration Point Orbits," *Journal of the Astronautical Sciences,* Vol. 42, No. 2, April-June 1994, pp. 207-228.

3 Gómez, G., Llibre, J., Martínez, R., and Simó, C., *Dynamics and Mission Design Near Libration Points, Vol. I: Fundamentals: The Case of Collinear Libration Points*, World Scientific Monograph Series, World Scientific Publishing Ltd., Singapore, 2001.

4. Howell, K.C., and Marchand. B.G., "Natural and Non-Natural Spacecraft Formations Near the L_1 and L_2 Libration Points in the Sun-Earth/Moon Ephemeris System," *Dynamical Systems: an International Journal,* Special Issue: "Dynamical Systems in Dynamical Astronomy and Space Mission Design," Vol. 20, No. 1, March 2005, pp. 149-173.

5. Renault, C., and Scheeres, D., "Statistical Analysis of Control Maneuvers in Unstable Orbital Environments," *Journal of Guidance, Control, and Dynamics*, Vol. 26, No. 5, September-October 2003, pp 758-769.

6. Woodard, M., Folta, D., and Woodfork, D., "ARTEMIS: The First Mission to the Lunar Libration Points," 21st International Symposium on Space Flight Dynamics, Toulouse, France September 28-October 2, 2009.

7. V. Angelopoulos and D. G. Sibeck, "THEMIS and ARTEMIS," a proposal submitted for the Senior Review 2008 of the Mission Operations and Data Analysis Program for the Heliophysics Operating Missions; available at
http://www.igpp.ucla.edu/public/THEMIS/SCI/Pubs/Proposals%20and%20Reports/-
HP SR 2008 THEMIS SciTech 20080221.pdf, 2005.

8. M. Bester, M. Lewis, B. Roberts, J. Thorsness, J. McDonald, D. Pease, S. Frey, and D. Cosgrove, Multi-mission Flight Operations at UC Berkeley – Experiences and Lessons Learned," AIAA 2010, SpaceOps Conference Papers on Disk, Huntsville, AL, April 25-30, 2010, Paper AIAA-2010-2198.

9. Broschart S., et al, "Preliminary Trajectory Design for the Artemis Lunar Mission", AAS 09-382, AAS/AIAA AstrodynamicsSpecialist Conference held August 9-13 2009,Pittsburgh, Pennsylvania.

10. W. S. Koon, M. W. Lo, J. E. Marsden, and S. D. Ross, "Heteroclinic Connections Between Periodic Orbits and Resonance Transitions in Celestial Mechanics," Chaos, Vol. 10, No. 2, 2000, pp. 427–469.

11. Gómez, G., Jorba, A., Masdemont, J., and Simó, C., "Study of the Transfer from the Earth to a Halo Orbit Around the Equilibrium Point L_1," *Celestial Mechanics and Dynamical Astronomy*, Vol. 56, No. 4, 1993, pp. 541-562.

12. Howell, K.C., Mains, D.L., and Barden, B.T., "Transfer Trajectories from Earth Parking Orbits to Sun-Earth Halo Orbits," *AAS/AIAA Space Flight Mechanics Meeting 1994*, Advances in the Astronautical Sciences, Vol. 87, J. Cochran, C. Edwards, S. Hoffman, and R. Holdaway (editors), 1994, pp. 399-422.

13. Barden, B.T., and Howell, K.C., "Fundamental Motions Near Collinear Libration Points and Their Transitions," *Journal of the Astronautical Sciences*, Vol. 46, No. 4, October-December 1998, pp. 361-378.

14. Belbruno, E.A., "Sun-perturbed Earth-to-Moon Transfers with Ballistic Capture. Journal of Guidance Control and Dynamics, 16(4): 770-775, 1993

15. Belbruno, E.A., "The Dynamical Mechanism of Ballistic lunar Capture Transfers in the Four Body Problem from the Perspective of Invariant manifolds and Hill's Regions", Institut D'Estudis Catalans CRM Research Report No.270.

16. Bello-Mora, M. F., Graziana P. T., et al, "A systematic Analysis on Weak Stability Boundary Transfers to the Moon. *In* Proc 51st International Astronautical Congress IAF-00-A.6.03, Rio de Janeiro, Brazil. 2000

17. Howell, K.C., Barden, B.T., and Lo, M.W., "Application of Dynamical Systems Theory to Trajectory Design for a Libration Point Mission," *Journal of the Astronautical Sciences*, Vol. 45, No. 2, April-June 1997, pp. 161-178.

18. Barden, B.T., Wilson, R.S., Howell, K.C., and Marchand, B.G., "Summer Launch Options for the Genesis Mission," AAS/AIAA Astrodynamics Specialists Conference, Quebec City, Canada, July 30 - August 2, 2001.